Lumped-parameter models

Ibsen, Lars Bo; Liingaard, Morten

Publication date:
2006

Document Version
Publisher's PDF, also known as Version of record

Lumped-parameter models

Lars Bo Ibsen
Morten Liingaard

ISSN 1901-726X
DCE Technical Report No. 11

AALBORG UNIVERSITY
Department of Civil Engineering

Aalborg University
Department of Civil Engineering
Division of Water and Soil

DCE Technical Report No. 11

Lumped-parameter models

by

Lars Bo Ibsen
Morten Liingaard

December 2006

Scientific Publications at the Department of Civil Engineering

Technical Reports are published for timely dissemination of research results and scientific work carried out at the Department of Civil Engineering (DCE) at Aalborg University. This medium allows publication of more detailed explanations and results than typically allowed in scientific journals.

Technical Memoranda are produced to enable the preliminary dissemination of scientific work by the personnel of the DCE where such release is deemed to be appropriate. Documents of this kind may be incomplete or temporary versions of papers—or part of continuing work. This should be kept in mind when references are given to publications of this kind.

Contract Reports are produced to report scientific work carried out under contract. Publications of this kind contain confidential matter and are reserved for the sponsors and the DCE. Therefore, Contract Reports are generally not available for public circulation.

Lecture Notes contain material produced by the lecturers at the DCE for educational purposes. This may be scientific notes, lecture books, example problems or manuals for laboratory work, or computer programs developed at the DCE.

Theses are monograms or collections of papers published to report the scientific work carried out at the DCE to obtain a degree as either PhD or Doctor of Technology. The thesis is publicly available after the defence of the degree.

Latest News is published to enable rapid communication of information about scientific work carried out at the DCE. This includes the status of research projects, developments in the laboratories, information about collaborative work and recent research results.

Published 2006 by
Aalborg University
Department of Civil Engineering
Sohngaardsholmsvej 57,
DK-9000 Aalborg, Denmark

Printed in Denmark at Aalborg University

ISSN 1901-726X
DCE Technical Report No. 11

Preface

The technical report "Lumped-parameter models" is divided into three numbered sections, and a list of references is situated after the last section. Tables, equations and figures are indicated with consecutive numbers. Cited references are marked as e.g. Houlsby and Cassidy (2002), with author specification and year of publication in the text.

The work within this report has only been possible with the financial support from the Energy Research Programme (ERP)[1] administered by the Danish Energy Authority. The project is associated with the ERP programme "Soil–Structure interaction of Foundations for Offshore Wind Turbines". The funding is sincerely acknowledged.

Aalborg, December 11, 2006 Lars Bo Ibsen & Morten Liingaard

[1] In danish: "Energiforskningsprogrammet (EFP)"

Contents

List of Figures

List of Tables

Chapter 1
Lumped-parameter models

A lumped-parameter model represents the frequency dependent soil-structure interaction of a massless foundation placed on or embedded into an unbounded soil domain. The lumped-parameter model development have been reported by (Wolf 1991b; Wolf 1991a; Wolf and Paronesso 1991; Wolf and Paronesso 1992; Wolf 1994; Wolf 1997; Wu and Lee 2002; Wu and Lee 2004).

In this technical report the the steps of establishing a lumped-parameter model are presented. Following sections are included in this report: Static and dynamic formulation (Section 1.1), Simple lumped-parameter models (Section 1.2) and Advanced lumped-parameter models (Section 1.3).

1.1 Static and Dynamic Stiffness Formulation

The elastic behaviour of foundations is relevant in several situations. The elastic response of footings is used to evaluate of deformations during working loads (in serviceability conditions) and may be used as the "elastic zone" for advanced elasto-plastic macro-models of foundations, see e.g. Martin and Houlsby (2001) and Houlsby and Cassidy (2002). The dynamic response of the wind turbine structure (e.g. eigen frequencies/modes) are affected by the properties of the foundation. The purpose of this research is to provide accurate means of evaluation of the dynamic properties of the foundation, so that it can be properly included in a composite structure-foundation system. The typical approach is that each analysis of the composite system should employ a complete analysis (using for instance finite-element method) of both the structure and foundation. Such an approach is, however, inefficient and time consuming, as for practical purposes the foundation system can be treated as a substructure with predetermined properties. The interactions between the foundation and structure are then expressed purely in terms of force and moment resultants, and their conjugate displacements and rotations, see Figure 1.1.

1.1.1 Static stiffness

The elastic static stiffness of the foundation can be expressed by dimensionless elastic stiffness coefficients corresponding to vertical (K^0_{VV}), horizontal (K^0_{HH}), moment (K^0_{MM}) and torsional (K^0_{TT}) degrees of freedom. Cross-coupling between horizontal and moment

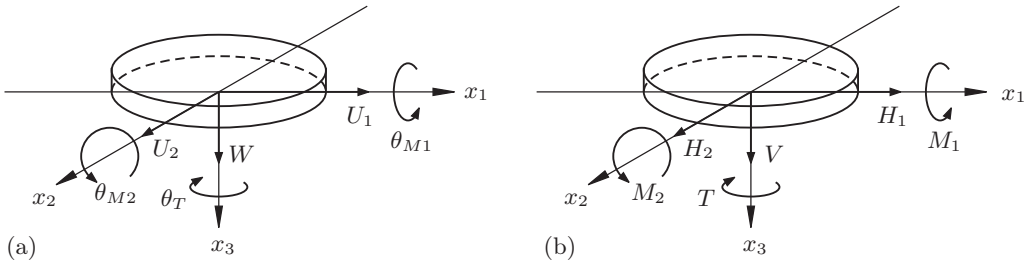

Figure 1.1: Degrees of freedom for a rigid surface footing: (a) displacements and rotations, and (b) forces and moments.

loads exists so an additional cross-coupling term (K^0_{MH}) is necessary. Under general (combined) static loading (see Figure 1.1) the elastic stiffness of the foundation system can be expressed as

$$\begin{bmatrix} V/G_sR^2 \\ H_1/G_sR^2 \\ H_2/G_sR^2 \\ T/G_sR^3 \\ M_1/G_sR^3 \\ M_2/G_sR^3 \end{bmatrix} = \begin{bmatrix} K^0_{VV} & 0 & 0 & 0 & 0 & 0 \\ 0 & K^0_{HH} & 0 & 0 & 0 & -K^0_{MH} \\ 0 & 0 & K^0_{HH} & 0 & K^0_{MH} & 0 \\ 0 & 0 & 0 & K^0_{TT} & 0 & 0 \\ 0 & 0 & K^0_{MH} & 0 & K^0_{MM} & 0 \\ 0 & -K^0_{MH} & 0 & 0 & 0 & K^0_{MM} \end{bmatrix} \begin{bmatrix} W/R \\ U_1/R \\ U_2/R \\ \theta_T \\ \theta_{M1} \\ \theta_{M2} \end{bmatrix}, \tag{1.1}$$

where R is the radius of the foundation and G_s is the shear modulus of the soil. The shear modulus G_s is given by

$$G_s = \frac{E_s}{2\,(1+\nu_s)} \tag{1.2}$$

where E_s is Young's modulus and ν_s is Poisson's ratio. Note that the foundation is assumed to be rigid and the soil is linear elastic, i.e. the properties are given by G_s and ν_s. This means that the stiffness components K^0_{ij} $(i,j = H,M,T,V)$ in 1.1 are functions of Poisson's ratio.

1.1.2 Dynamic stiffness

It is assumed that the foundation is excited with a harmonic vibrating force with the circular frequency ω. The dynamic system for a vertical vibrating surface footing with no mass is shown in Figure 1.2(a). For each degree of freedom the dynamic stiffness of the system can be represented by a frequency dependent spring and dashpot, as shown in Figure 1.2(b).

A generalized massless axisymmetric rigid foundation has six degrees of freedom: one vertical, two horizontal, two rocking and one torsional. The six degrees of freedom and the corresponding forces and moments are shown in Figure 1.1. The dynamic stiffness matrix $\mathbf{S}$ is related to the vector of forces and moments $\mathbf{R}$ and the vector of displacements and rotations $\mathbf{U}$ as follows:

$$\mathbf{R} = \mathbf{S}\mathbf{U} \tag{1.3}$$

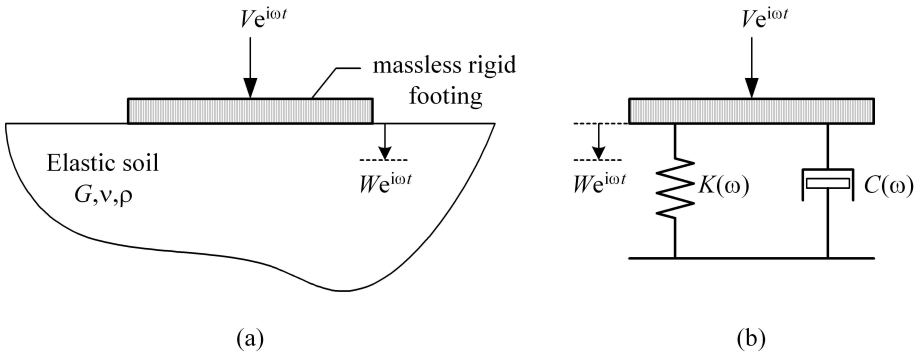

Figure 1.2: (a) Vertical vibrating surface footing resting on a homogeneous elastic half-space. (b) Analogy for dynamic soil response.

The component form of Equation (1.3) can be written as:

$$\begin{bmatrix} V/G_sR^2 \\ H_1/G_sR^2 \\ H_2/G_sR^2 \\ T/G_sR^3 \\ M_1/G_sR^3 \\ M_2/G_sR^3 \end{bmatrix} = \begin{bmatrix} S_{VV} & 0 & 0 & 0 & 0 & 0 \\ 0 & S_{HH} & 0 & 0 & 0 & -S_{MH} \\ 0 & 0 & S_{HH} & 0 & S_{MH} & 0 \\ 0 & 0 & 0 & S_{TT} & 0 & 0 \\ 0 & 0 & S_{MH} & 0 & S_{MM} & 0 \\ 0 & -S_{MH} & 0 & 0 & 0 & S_{MM} \end{bmatrix} \begin{bmatrix} W/R \\ U_1/R \\ U_2/R \\ \theta_T \\ \theta_{M1} \\ \theta_{M2} \end{bmatrix} \tag{1.4}$$

where R is the radius of the foundation and G_s is the shear modulus of the soil. The components in $\mathbf{S}$ are functions of the cyclic frequency ω, and $\mathbf{S}$ reflects the dynamic stiffness of the soil for a given shape of the foundation. The components of $\mathbf{S}$ can be written as:

$$S_{ij}(\omega) = K_{ij}(\omega) + \mathrm{i}\omega C_{ij}(\omega), \qquad (i,j = H,M,T,V), \tag{1.5}$$

where K_{ij} and C_{ij} are the dynamic stiffness and damping coefficients with respect to ω, respectively, and i is the imaginary unit, $\mathrm{i} = \sqrt{-1}$. It is convenient to use dimensionless frequency $a_0 = \omega R/c_S$ that is normalized by the ratio of the foundation radius R and the shear wave velocity of the soil c_S. The dynamic stiffness components can then be written as

$$S_{ij}(a_0) = K_{ij}^0 \left[k_{ij}(a_0) + \mathrm{i}a_0 c_{ij}(a_0)\right], \qquad (i,j = H,M,T,V), \tag{1.6}$$

where K_{ij}^0 is the static value of ijth stiffness component, k_{ij} and c_{ij} are the dynamic stiffness and damping coefficients with respect to a_0, respectively. The non-dimensional dynamic stiffness and damping coefficients, k_{ij} and c_{ij}, are both real. Both geometrical damping, i.e. the radiation of waves into the subsoil, and possibly also material dissipation contribute to c_{ij}.

In some situations it is useful to examine the magnitude and phase angle of Equation (1.6) in addition to the real and imaginary parts of the dynamic stiffness. The

magnitude (complex modulus) of S_{ij} is given by

$$|S_{ij}| = |K_{ij}^0| \sqrt{(k_{ij})^2 + (a_0 c_{ij})^2}, \tag{1.7}$$

and the phase angle ϕ_{ij} of S_{ij} is given as

$$\phi_{ij} = \arctan\left(\frac{a_0 c_{ij}}{k_{ij}}\right). \tag{1.8}$$

Note that the above-mentioned stiffness formulations are based on the fact that the foundation is rigid. This means that components in $\mathbf{S}$ are functions of Poisson's ratio ν_s and the circular frequency ω (if dynamic) for a given shape of the foundation.

1.2 Simple lumped-parameter models

The frequency dependency of the foundation stiffness is taken into account, by applying lumped-parameter models. Two types of models are categorized as simple models: The standard lumped-parameter model and the fundamental lumped-parameter model. The presentation of the models is based on Wolf (1994).

1.2.1 Standard lumped-parameter model

The standard lumped-parameter model contains three coefficients, K, C and M, for each degree of freedom, see Figure 1.3. The spring stiffness K is equal to the static stiffness coefficient for the elastic half-space, thus K is given by the expressions in section 1.1.1. The dashpot and mass coefficients, C and M, do not have physical meaning but are solely curve fitting parameters, used to reproduce the dynamic stiffness of the foundation. The parameters C and M are given by two non-dimensional coefficients γ and μ by

$$C = \frac{R}{c_S}\gamma K \tag{1.9a}$$

$$M = \frac{R^2}{c_S^2}\mu K. \tag{1.9b}$$

The values of K, γ and μ for a circular disk with mass on a elastic half-space are given in Table 1.1 (Reproduced from Wolf (1994)).

Note that the inertia of the disk m (mass moment of inertia for rocking vibrations) enters the expressions for γ with respect to rocking and torsional vibrations in the expressions given by Wolf (1994). However, it is possible to construct the parameters for a massless foundation.

Based on the three coefficients, K, C and M, the dynamic stiffness for a each degree of freedom can be formulated as

$$S(\omega) = K - \omega^2 M + \mathrm{i}\omega C. \tag{1.10}$$

The dynamic stiffness in Equation (1.10) can be rewritten in terms of the non-dimensional frequency a_0 as

$$S(a_0) = K\left[k(a_0) + \mathrm{i}a_0 c(a_0)\right]. \tag{1.11}$$

Table 1.1: Non-dimensional coefficients for the standard lumped-parameter model. The coefficients corresponds to a disk with mass on an elastic half-space.

	Static stiffness K	Dashpot coeff. γ	Mass coeff. μ
Horizontal	$\frac{8G_sR}{2-\nu_s}$	0.58	0.095
Vertical	$\frac{4G_sR}{1-\nu_s}$	0.85	0.27
Rocking	$\frac{8G_sR^3}{3(1-\nu_s)}$	$\frac{0.3}{1+\frac{3(1-\nu_s)m}{8R^5\rho_s}}$	0.24
Torsional	$\frac{16G_sR^3}{3}$	$\frac{0.433}{1+\frac{2m}{R^5\rho_s}}\sqrt{\frac{m}{R^5\rho_s}}$	0.045

By comparing Equations (1.9) and (1.10) with Equation (1.11) it becomes evident that the spring and damping coefficients $k(a_0)$ and $c(a_0)$ can be written as

$$k(a_0) = 1 - \mu a_0^2 \tag{1.12a}$$

$$c(a_0) = \gamma. \tag{1.12b}$$

It turns out that the damping term $c(a_0)$ of the standard lumped-parameter model is constant. This behaviour is not well suited to represent the damping of a footing, in particular with respect to the torsional and rocking vibrations. Further, the normalized real part of Equation (1.11) given by $k(a_0)$ in Equation (1.12) describes a parabolic shape of the dynamic stiffness. The parabolic shape may represent the actual dynamic stiffness of a given foundation at low frequencies, but is inadequate for modelling the dynamic stiffness at intermediate and high frequencies. The standard lumped-parameter approximation of the vertical dynamic stiffness of a massless circular rigid footing is illustrated in Figure 1.4. The approximation is compared with a rigorous solution provided by Veletsos and Tang (1987).

The main advantage of the standard lumped-parameter is that no additional degrees of freedom are introduced. However, the frequency dependent representation of the dynamic stiffness is very simple. Thus, the model is restricted to be used in the low-

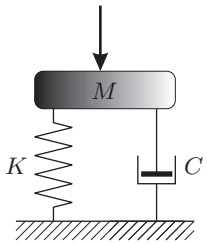

Figure 1.3: Standard lumped-parameter model for translation motion.

frequency range.

1.2.2 Fundamental lumped-parameter models

The fundamental lumped-parameter model consists of one static stiffness parameter and four free parameters, found by curve fitting. As opposed to the standard lumped-parameter model, this type of model contains one additional internal degree of freedom. The fundamental lumped-parameter model can assembled in several ways by combining spring, dashpots and masses. Two examples are shown in Figure 1.5. The spring stiffness K is equal to the static stiffness coefficient for the elastic half-space, given by the expressions in section 1.1.1. The remaining four *free parameters* are obtained by curve fitting. The spring-dashpot model in Figure 1.5a is represented by the parameters M_0, C_0, K_1 and C_1, whereas the monkey-tail model in Figure 1.5b is represented by the parameters M_0, C_0, M_1 and C_1. Consider the monkey-tail model. The four free parameters M_0, C_0, M_1 and C_1 can be formulated by means of the non-dimensional coefficients μ_0, γ_0, μ_1 and γ_1 as

$$M_0 = \frac{R^2}{c_S^2}\mu_0 K \tag{1.13a}$$

$$C_0 = \frac{R}{c_S}\gamma_0 K \tag{1.13b}$$

$$M_1 = \frac{R^2}{c_S^2}\mu_1 K \tag{1.13c}$$

$$C_1 = \frac{R}{c_S}\gamma_1 K \tag{1.13d}$$

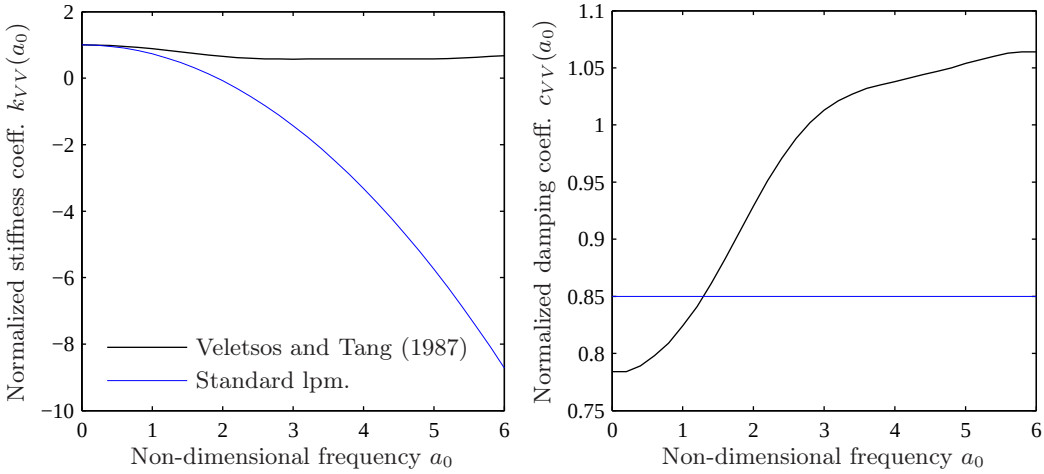

Figure 1.4: Vertical dynamic stiffness of a massless circular footing on an elastic half-space. The rigorous solution is compared with the approximation of a standard lumped-parameter model.

Table 1.2: Non-dimensional coefficients for the fundamental lumped-parameter model. The coefficients correspond to a disk on an elastic half-space.

	Static stiffness	Dashpots		Masses		
	K	γ_0	γ_1	μ_0		μ_1
Horizontal	$\frac{8G_sR}{2-\nu_s}$	0.78-0.4ν_s	—	—		—
Vertical	$\frac{4G_sR}{1-\nu_s}$	0.8	0.34-4.3ν_s^4	$\nu_s < \frac{1}{3}$	0	0.4-4ν_s^4
				$\nu_s > \frac{1}{3}$	0.9$(\nu_s - \frac{1}{3})$	
Rocking	$\frac{8G_sR^3}{3(1-\nu_s)}$	—	0.42-0.3ν_s^2	$\nu_s < \frac{1}{3}$	0	0.34-0.2ν_s^2
				$\nu_s > \frac{1}{3}$	0.16$(\nu_s - \frac{1}{3})$	
Torsional	$\frac{16G_sR^3}{3}$	0.017	0.291	—		0.171

The values of K, μ_0, γ_0, μ_1 and γ_1 for a circular disk on a elastic half-space are given in Table 1.2 (Reproduced from Wolf (1994)). Most of the coefficients, except for torsional vibrations, depend on ν_s. Note that some of the non-dimensional coefficients may be missing for some of the vibration modes.

The dynamic stiffness $S(\omega)$ of the fundamental lumped-parameter model (for harmonic loading) can be established by formulating the equilibrium equation for each of the two degrees of freedom, $u_0(\omega)$ and $u_1(\omega)$ in Figure 1.5b. The two equilibrium equations are

$$-\omega^2 M_1 u_1(\omega) + \mathrm{i}\omega C_1 \left[u_1(\omega) - u_0(\omega)\right] = 0, \tag{1.14a}$$

$$-\omega^2 M_0 u_0(\omega) + \mathrm{i}\omega \left(C_0 + C_1\right) u_0(\omega) - \mathrm{i}\omega C_1 u_1(\omega) + K u_0(\omega) = P_0(\omega), \tag{1.14b}$$

where $u_0(\omega)$ is the displacement amplitude related to the applied load amplitude $P_0(\omega)$. By eliminating $u_1(\omega)$ in Equations (1.14a) and (1.14b) the relation between $P_0(\omega)$ and

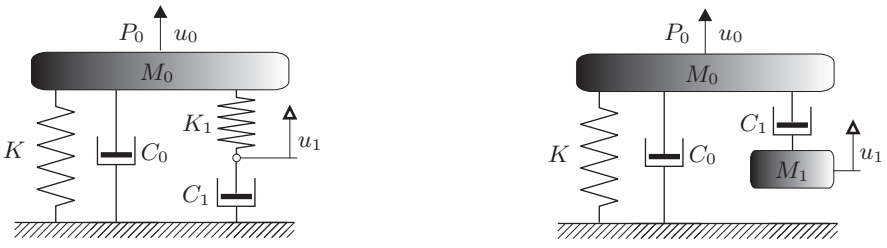

Figure 1.5: Fundamental lumped-parameter models. (a) Spring-dashpot model, and (b) monkey-tail model.

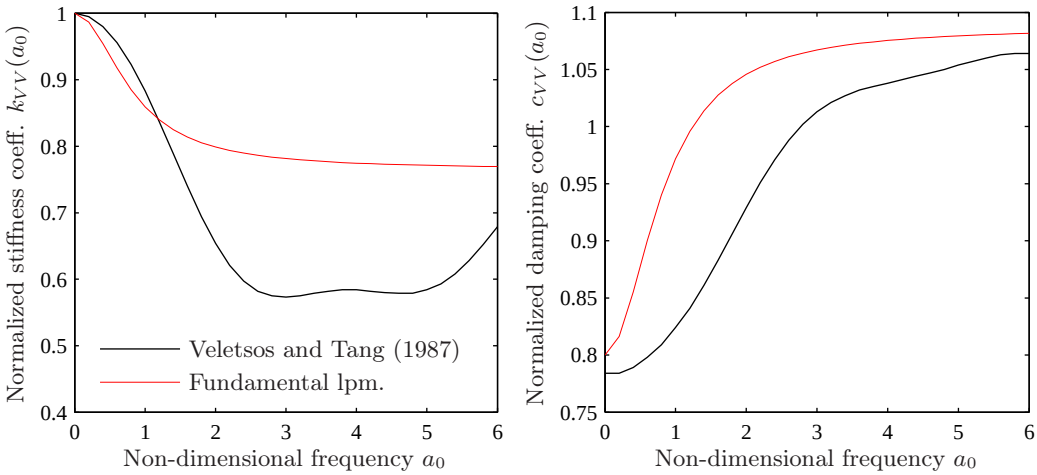

Figure 1.6: Vertical dynamic stiffness of a massless circular footing on an elastic half-space. The rigorous solution is compared with the approximation of a fundamental lumped-parameter model.

$u_0(\omega)$ is given as

$$P_0(\omega) = \underbrace{K\left[1 - \frac{\frac{\omega^2 M_1}{K}}{1+\frac{\omega^2 M_1^2}{C_1^2}} - \frac{\omega^2 M_0}{K} + \mathrm{i}\omega\left(\frac{M_1}{C_1}\frac{\frac{\omega^2 M_1}{K}}{1+\frac{\omega^2 M_1^2}{C_1^2}} + \frac{C_0}{K}\right)\right]}_{S(\omega)} u_0(\omega). \tag{1.15}$$

The dynamic stiffness in Equation (1.15) can be rewritten in terms of the non-dimensional frequency a_0 as stated in Equation (1.11). By substituting Equation (1.13) into Equation (1.15), the spring and damping coefficients $k(a_0)$ and $c(a_0)$ of the fundamental lumped-parameter model (monkey-tail version) can determined as

$$k(a_0) = 1 - \frac{\mu_1 a_0^2}{1+\frac{\mu_1^2}{\gamma_1^2}a_0^2} - \mu_0 a_0^2 \tag{1.16a}$$

$$c(a_0) = \frac{\mu_1}{\gamma_1}\frac{\mu_1 a_0^2}{1+\frac{\mu_1^2}{\gamma_1^2}a_0^2} + \gamma_0. \tag{1.16b}$$

As opposed to the standard lumped-parameter model, the fundamental lumped-parameter model is double-asymptotic, meaning that the approximation of $S(a_0)$ is exact for the static limit, $a_0 \to 0$, and for the high-frequency limit, for $a_0 \to \infty$. The fundamental lumped-parameter approximation of the vertical dynamic stiffness of a massless circular rigid footing is illustrated in Figure 1.6. The approximation is compared with a rigorous solution provided by Veletsos and Tang (1987). By including an additional degree of freedom this approximation has approved when comparing with the standard lumped-parameter model in the previous section. Note that the procedure for establishing the formulation for spring-dashpot model is similar to that of the monkey-tail model. The only difference is the characteristics of the non-dimensional coefficients.

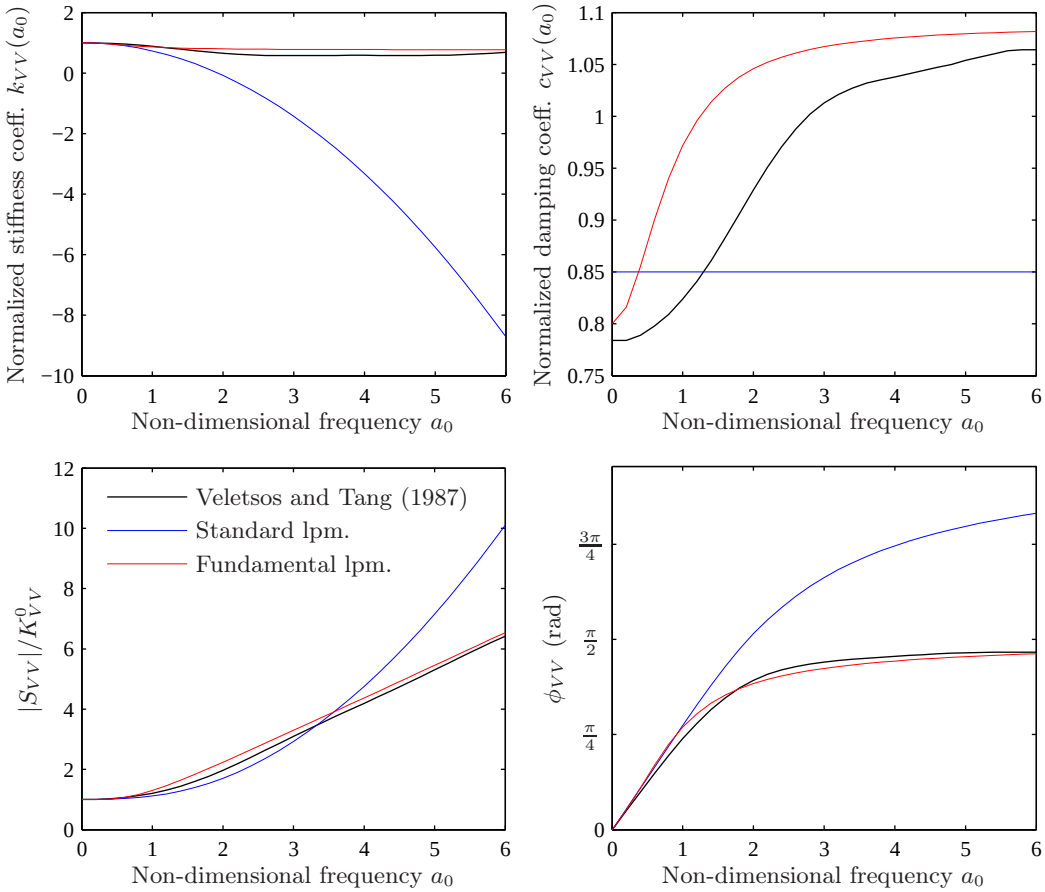

Figure 1.7: Vertical dynamic stiffness of a massless circular footing on an elastic half-space. The rigorous solution is compared with the approximation of both the standard and the fundamental lumped-parameter model.

The approximation of the fundamental lumped-parameter model is compared with that of the standard lumped-parameter model in Figure 1.7. The approximations are shown for the real and imaginary part of the dynamic stiffness, as well as for the magnitude and phase angle.

1.3 Advanced lumped-parameter models

The investigations of frequency dependent behaviour of massless foundations often involves complicated three-dimensional elastodynamic analyses using rigorous methods, such as the finite element method or the boundary element method. The employed models typically consist of several thousand degrees of freedom, and the frequency dependent dynamic stiffness of the foundations are evaluated in the frequency domain. The requirement for real-time computations in the time domain in aero-elastic codes do not conform with the use of e.g. a three-dimensional coupled Boundary Element/Finite Element Method, where the foundation stiffness is evaluated in the frequency domain.

In order to meet the requirements of real-time calculations and analysis in time domain, lumped-parameter models are particularly useful. A lumped-parameter model represents a unbounded soil domain, and the soil-structure interaction of a massless foundation can be modelled by relatively few springs, dashpots and masses, all with real frequency-independent coefficients. Each degree of freedom at the foundation node of the structural model is coupled to a lumped-parameter model that may consist of additional internal degrees of freedom. A systematic procedure to obtain consistent lumped-parameter models with real coefficients has been suggested by Wolf (1991b). The procedure is as follows:

- Determine the frequency dependent impedance or dynamic stiffness $S(a_0)$ by means of the finite element method or the boundary element method.
- Decompose the dynamic stiffness $S(a_0)$ into a singular part $S_s(a_0)$ and a regular part $S_r(a_0)$. The singular part $S_s(a_0)$ represents the asymptotic value of the dynamic stiffness for $a_0 \to \infty$. The difference between $S(a_0)$ and $S_s(a_0)$ is the regular part $S_r(a_0)$.
- Approximate the regular part $S_r(a_0)$ by the ratio of two polynomials P and Q. The degree of the polynomial in the denominator is M and one less $(M-1)$ in the the numerator. The approximation of the regular part $S_r(a_0)$ now contains $2M-1$ unknown real coefficients, which are determined by a curve-fitting technique based on the least-squares method.
- Establish the lumped-parameter model from the $2M-1$ real coefficients. The lumped-parameter model may contain several constant/linear, first-order and second-order discrete-element models. Finally, the lumped-parameter model is formulated into stiffness, damping and mass matrices, which can be incorporated into standard dynamic programs.

The four steps in the procedure are explained in the following sections. It should be noted that the lumped-parameter models do not provide any information of the stresses or strains in the embedded foundations or in the surrounding subsoil. The models are macro-models of the entire soil-structure interface.

1.3.1 Dynamic stiffness obtained from rigorous methods

The classical methods for analysing vibrations of foundations are based on analytical solutions for massless circular foundations resting on an elastic half-space. The classical

solutions by Reissner, Quinlan and Sung were obtained by integration of Lamb's solution for a vibrating point load on a half-space (Richart et al. 1970; Das 1993). The mixed boundary value problems with prescribed conditions under the foundation and zero traction at the remaining free surface were investigated by Veletsos and Wei (1971) and Luco and Westmann (1971). The integral equations of the mixed boundary value problems were evaluated and tabulated for a number of excitation frequencies. A closed-form solution has been presented by Krenk and Schmidt (1981).

Whereas analytical and semi-analytical solutions may be formulated for surface footings with a simple geometries, numerical analysis is required in the case of flexible embedded foundations with complex geometry. The Finite Element Method (FEM) is very useful for the analysis of structure with local inhomogeneities and complex geometries. However, only a finite region can be discretized. Hence, at the artificial boundaries of the unbounded domain, e.g. soil, transmitting boundary conditions must be applied as suggested by Higdon (1990), Higdon (1992) and Krenk (2002). Numerous concepts, including the Scaled Boundary Finite Element Method are presented by Wolf and Song (1996), and Andersen (2002) gave a brief overview of different solutions techniques. In the case of analyses by coupled boundary element/finite element models, wave radiation into the subsoil is ensured by a coupling with the boundary element method. If the full-space fundamental solution is utilized, both the soil–foundation interface and the free soil surface must be discretized. A smaller numerical model, i.e. a model with fewer degrees of freedom, may be obtained with the use of other types of solutions, e.g. half-space solutions. However, this comes at the cost that the fundamental solution can be very complicated, and often a closed-form solution cannot be found. The work within the boundary element formulation of dynamic soil–structure interaction has been reported by, for example, Domínguez (1993), Beskos (1987) and Beskos (1997).

1.3.2 Decomposition of the dynamic stiffness

The complex frequency dependent dynamic stiffness coefficient for each degree of freedom is denoted by $S(a_0)$. In the following the indices are omitted for simplicity. $S(a_0)$ are then decomposed into a singular part $S_s(a_0)$, and a regular part $S_r(a_0)$, given by

$$S\left(a_0\right) = S_s\left(a_0\right) + S_r\left(a_0\right), \tag{1.17}$$

where

$$S_s\left(a_0\right) = K^0\left[k^\infty + \mathrm{i}a_0 c^\infty\right]. \tag{1.18}$$

For the limit $a_0 \to \infty$, the second term on the right-hand side dominates, leading to a high-frequency limit

$$S_s\left(a_0\right) \approx K^0\left[\mathrm{i}a_0 c^\infty\right]. \tag{1.19}$$

The high-frequency behaviour of a surface footing is characterized by a phase angle approaching $\pi/2$ for $a_0 \to \infty$ and a linear relation that passes through origo in a frequency vs. magnitude diagram. The slope of the curve is equal to a limiting damping parameter c^∞ that describes the impedance for $a_0 \to \infty$. For example, the vertical limiting damping

parameter in terms of ω of a circular surface footing is given by

$$C_{VV}^{\infty} = \rho_s c_P A_b, \tag{1.20}$$

where A_b is the area of the base of the foundation. The vertical limiting damping parameter in terms of a_0 can be found by multiplying by the right-hand side in Equation (1.20) by $\frac{c_S}{K^0 R}$ (Recall that $a_0 = \omega R/c_S$). The vertical limiting damping parameter c_{VV}^{∞} is then given as

$$c_{VV}^{\infty} = [\rho_s c_P A_b] \frac{c_S}{K^0 R}. \tag{1.21}$$

It should be noted that C_{VV}^{∞} or c_{VV}^{∞} are highly sensitive to ν_s due to the fact that c_P enters the equation. For that reason c_P may be inappropriate, and Gazetas and Dobry (1984) suggest the use of *Lysmer's analog* 'wave velocity' c_{La}=$3.4c_S/\pi(1-\nu_s)$. Wolf (1994) suggests another approach where c_P for $\nu_s \in [1/3;0.5]$ is constant, and equal to c_P at $\nu_s = 1/3$.

Note that the singular part $S_s(a_0)$ is relatively simple to determine. $S_s(a_0)$ is a function of the mass density of the soil, the wave velocity of the soil, and the base area or moment of inertia of the foundation. The base area enters the equation for translational degrees of freedom, whereas the moment of inertia and the polar moment of inertia enters for the rocking and the torsional degree of freedom, respectively.

The remaining part $S_r(a_0)$ is found by subtracting $S_s(a_0)$ from $S(a_0)$. The regular part is used as input for the curve-fitting procedure described in the next section.

1.3.3 Polynomial-fraction approximation

The regular part $S_r(a_0)$ of the dynamic stiffness is approximated by the ratio of two polynomials P and Q. Furthermore, it is assumed that the polynomial-fraction approximation can be established in terms of $\mathrm{i}a_0$. The approximation of $S_r(a_0)$ in terms of P and Q is then

$$S_r(a_0) \approx S_r(\mathrm{i}a_0) = \frac{P(\mathrm{i}a_0)}{Q(\mathrm{i}a_0)} = K^0 \frac{\frac{K^0-k^{\infty}}{K^0} + p_1(\mathrm{i}a_0) + p_2(\mathrm{i}a_0)^2 + \cdots + p_{M-1}(\mathrm{i}a_0)^{M-1}}{1 + q_1(\mathrm{i}a_0) + q_2(\mathrm{i}a_0)^2 + \cdots + q_M(\mathrm{i}a_0)^M}, \tag{1.22}$$

where p_i, q_i are the $2M-1$ unknown real coefficients to be determined by curve-fitting. Note that the degree of the polynomial in the denominator is M, and $M-1$ in the the numerator.

The total approximation of $S(a_0)$ is found by adding Equations (1.18) and (1.22) as stated in Equation (1.17). The approximation has two important characteristics: The approximation of $S(a_0)$ is exact for the static limit, where $S(a_0) \to K^0$ for $a_0 \to 0$, and for the high-frequency limit, where $S(a_0) \to S_s(a_0)$ for $a_0 \to \infty$, since $S_r(a_0) \to 0$ for $a_0 \to \infty$. This means that the approximation is double-asymptotic.

The $2M-1$ unknown real coefficients in Equation (1.22) are computed by a MATLAB routine. The inputs are: the complex values of $S_r(a_0)$, the corresponding frequencies, and the degrees of the polynomials in the denominator and the numerator of Equation (1.22). The routine returns the real coefficients p_i, q_i of $S_r(a_0)$.

1.3.4 Discrete models for partial-fraction expansions

The polynomial-fraction approximation in Equation (1.22) can be formulated by a partial-fraction expansion, given by

$$\frac{S_r(\mathrm{i}a_0)}{K^0} = \sum_{l=1}^{M} \frac{A_l}{\mathrm{i}a_0 - s_l}, \tag{1.23}$$

where s_l are the poles of $S_r(\mathrm{i}a_0)$, and A_l are the residues at the poles. In order to obtain a stable system, the real part of the all the poles must be negative, otherwise the approximation may become unstable. This criterium can be handled by using an iterative algorithm to find a stable approximation to the system.

The polynomial coefficients p_i, q_i of Equation (1.22) can be converted into a partial-fraction expansion by routines in e.g. MATLAB (use the function `residue` that converts between partial-fraction expansion and polynomial coefficients). Some of the poles s_l may be complex, resulting in complex conjugate pairs of s_l. Consequently, the corresponding residues A_l also appear as complex conjugate pairs. When two complex conjugate pairs are added, a second-order term with real coefficients appears. For J conjugate pairs, Equation (1.23) can be rewritten as

$$\frac{S_r(\mathrm{i}a_0)}{K^0} = \sum_{l=1}^{J} \frac{\beta_{1l}\mathrm{i}a_0 + \beta_{0l}}{(\mathrm{i}a_0)^2 + \alpha_{1l}\mathrm{i}a_0 + \alpha_{0l}} + \sum_{l=1}^{M-2J} \frac{A_l}{\mathrm{i}a_0 - s_l}. \tag{1.24}$$

The coefficients α_{0l}, α_{1l}, β_{0l} and β_{1l} are given by

$$\alpha_{0l} = s_{1l}^2 + s_{2l}^2 \tag{1.25a}$$
$$\alpha_{1l} = -2s_{1l} \tag{1.25b}$$
$$\beta_{0l} = -2(A_{1l}s_{1l} + A_{2l}s_{2l}) \tag{1.25c}$$
$$\beta_{1l} = 2A_{1l}, \tag{1.25d}$$

where the real and imaginary parts of the complex conjugate poles are denoted by s_{1l} and s_{2l}, respectively. Similar, real and imaginary parts of the complex conjugate residues are denoted by A_{1l} and A_{2l}, respectively.

By adding the singular term in Equation (1.18) to the expression in Equation (1.23), the total approximation of the dynamic stiffness can be written as

$$\frac{S(\mathrm{i}a_0)}{K^0} = k^\infty + \mathrm{i}a_0 c^\infty + \sum_{l=1}^{J} \frac{\beta_{1l}\mathrm{i}a_0 + \beta_{0l}}{(\mathrm{i}a_0)^2 + \alpha_{1l}\mathrm{i}a_0 + \alpha_{0l}} + \sum_{l=1}^{M-2J} \frac{A_l}{\mathrm{i}a_0 - s_l}. \tag{1.26}$$

The total approximation of the dynamic stiffness in Equation (1.26) consists three characteristic types of terms: a constant/linear term, first-order terms and second-order terms. These terms are given as

$$\text{Constant/linear term} \qquad k^\infty + \mathrm{i}a_0 c^\infty \tag{1.27a}$$
$$\text{First-order term} \qquad \frac{A}{\mathrm{i}a_0 - s} \tag{1.27b}$$
$$\text{Second-order term} \qquad \frac{\beta_1 \mathrm{i}a_0 + \beta_0}{(\mathrm{i}a_0)^2 + \alpha_1 \mathrm{i}a_0 + \alpha_0}. \tag{1.27c}$$

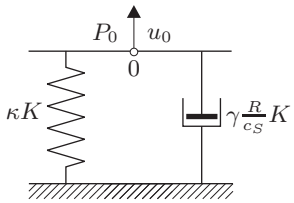

Figure 1.8: The discrete-element model for the constant/linear term.

The number of first- or second-order terms in the approximation depends on the choice of polynomial degree M. Each term can be represented by a discrete-element model, similar to those in Figures 1.3 and 1.5. The discrete-element models for the three types of terms in equation (1.27) are introduced in the next subsections.

Constant/linear term

The constant/linear term given by Equation (1.27a) consists of two known parameters, k^∞ and c^∞, that represents the singular part of the dynamic stiffness. The discrete-element model for the constant/linear term is shown in Figure 1.8. The equilibrium formulation of node 0 (for harmonic loading) is as follows

$$[\kappa K]\, u_0(\omega) + \mathrm{i}\omega \left[\gamma \frac{R}{c_S} K\right] u_0(\omega) = P_0(\omega) \tag{1.28}$$

Recalling that $a_0 = \omega R/c_S$ the equilibrium formulation in Equation (1.28) results in a force-displacement relation given by

$$\frac{P_0(a_0)}{K} = (\kappa + \mathrm{i}a_0\gamma)\, u_0(a_0). \tag{1.29}$$

By comparing Equation (1.27a) and Equation (1.29) it is evident that the non-dimensional coefficients, κ and γ, are equal to k^∞ and c^∞, respectively.

First-order term

The first-order term given by Equation (1.27b). The model has two known parameters, A and s. The layout of the discrete-element model is shown in Figure 1.9(a). The model is constructed by a spring $(-\kappa K)$ in parallel with another spring (κK) and dashpot $(\gamma\frac{R}{c_S}K)$ in series. The serial connection between the spring (κK) and the dashpot $(\gamma\frac{R}{c_S}K)$ results in an internal node 1 (internal degree of freedom). The equilibrium formulations for node 0 and 1 (for harmonic loading) are as follows

$$\text{node } 0: \qquad [\kappa K]\,\big(u_0(\omega) - u_1(\omega)\big) + [-\kappa K]\, u_0(\omega) = P_0(\omega) \tag{1.30a}$$

$$\text{node } 1: \qquad [\kappa K]\,\big(u_1(\omega) - u_0(\omega)\big) + \mathrm{i}\omega \left[\gamma \frac{R}{c_S} K\right] u_1(\omega) = 0. \tag{1.30b}$$

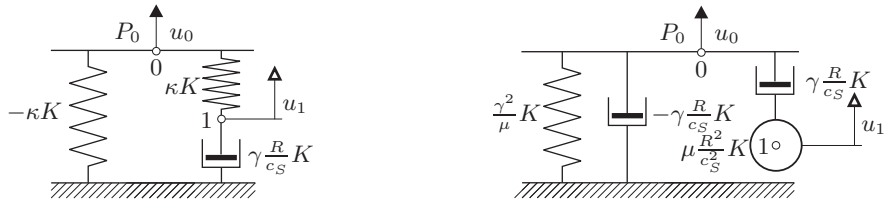

(a) (b)

Figure 1.9: The discrete-element model for the first-order term. (a) Spring-dashpot model, and (b) monkey-tail model.

By eliminating $u_1(\omega)$ in Equations (1.30a) and (1.30b) the force-displacement relation of the first-order model is given by

$$\frac{P_0(a_0)}{K} = \frac{-\frac{\kappa^2}{\gamma}}{\mathrm{i}a_0 + \frac{\kappa}{\gamma}} u_0(a_0). \tag{1.31}$$

By comparing Equations (1.27b) and (1.31) κ and γ are identified as

$$\kappa = \frac{A}{s} \tag{1.32a}$$

$$\gamma = -\frac{A}{s^2}. \tag{1.32b}$$

It should be noted that the first-order term also could be represented by a monkey-tail model. This turns out to be advantageous in situations where κ and γ in Equation (1.32) are negative, which may be the case when A is positive (s is negative). To avoid negative coefficients of springs and dashpots, the monkey-tail model is applied, and the resulting coefficients are positive. By inspecting the equilibrium formulations for node 0 and 1, see Figure 1.9(b), the coefficients can be identified as

$$\gamma = \frac{A}{s^2} \tag{1.33a}$$

$$\mu = -\frac{A}{s^3}. \tag{1.33b}$$

Second-order term

The second-order term given by Equation (1.27c). The model has four known parameters, α_0, α_1, β_0 and β_1. An example of a second-order discrete-element model is shown in Figure 1.10(a). This particular model has two internal nodes. The equilibrium formulations

for nodes 0, 1 and 2 (for harmonic loading) are as follows

$$\text{node } 0: \qquad [\kappa_1 K]\big(u_0(\omega) - u_1(\omega)\big) + [-\kappa_1 K]\, u_0(\omega) = P_0(\omega) \tag{1.34a}$$

$$\text{node } 1: \qquad [\kappa_1 K]\big(u_1(\omega) - u_0(\omega)\big) + \mathrm{i}\omega\left[\gamma_1 \frac{R}{c_S} K\right]\big(u_1(\omega) - u_2(\omega)\big) = 0 \tag{1.34b}$$

$$\text{node } 2: \qquad [\kappa_2 K]\, u_2(\omega) + \mathrm{i}\omega\left[\gamma_2 \frac{R}{c_S} K\right] u_2(\omega) + \mathrm{i}\omega\left[\gamma_1 \frac{R}{c_S} K\right]\big(u_2(\omega) - u_1(\omega)\big) = 0. \tag{1.34c}$$

After some rearrangement and elimination the internal degrees of freedom, the force-displacement relation of the second-order model is given by

$$\frac{P_0(a_0)}{K} = \frac{-\kappa_1^2 \frac{\gamma_1+\gamma_2}{\gamma_1\gamma_2}\mathrm{i}a_0 - \frac{\kappa_1^2\kappa_2}{\gamma_1\gamma_2}}{(\mathrm{i}a_0)^2 + \left(\kappa_1 \frac{\gamma_1+\gamma_2}{\gamma_1\gamma_2} + \frac{\kappa_2}{\gamma_2}\right)\mathrm{i}a_0 + \frac{\kappa_1\kappa_2}{\gamma_1\gamma_2}} u_0(a_0). \tag{1.35}$$

The four coefficients in Equation (1.35) can be identified as

$$\kappa_1 = -\frac{\beta_0}{\alpha_0} \tag{1.36a}$$

$$\gamma_1 = -\frac{\alpha_0\beta_1 - \alpha_1\beta_0}{\alpha_0^2} \tag{1.36b}$$

$$\kappa_2 = \frac{\beta_0}{\alpha_0^2}\frac{(-\alpha_0\beta_1 + \alpha_1\beta_0)^2}{\alpha_0\beta_1^2 - \alpha_1\beta_0\beta_1 + \beta_0^2} \tag{1.36c}$$

$$\gamma_2 = \frac{\beta_0^2}{\alpha_0^2}\frac{-\alpha_0\beta_1 + \alpha_1\beta_0}{\alpha_0\beta_1^2 - \alpha_1\beta_0\beta_1 + \beta_0^2}, \tag{1.36d}$$

by comparison of Equations (1.27c) and (1.35).

By introducing a second-order model with springs, dampers and a mass, it is possible to construct a second-order model with only one internal degree of freedom. The model

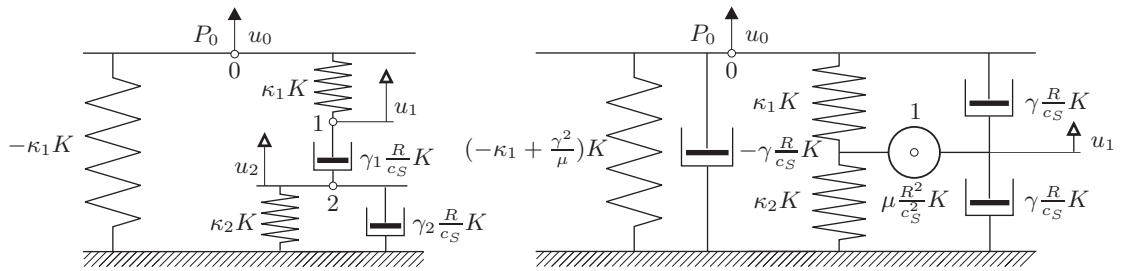

Figure 1.10: The discrete-element model for the second-order term. (a) Spring-dashpot model with two internal degrees of freedom, and (b) Spring-dashpot-mass model with one internal degree of freedom.

is sketched in Figure 1.10(b). The force-displacement relation of the alternative second-order model is given by

$$\frac{P_0(a_0)}{K} = \frac{2\left(\frac{\kappa_1\gamma}{\mu} + \frac{\gamma^3}{\mu^2}\right)\mathrm{i}a_0 - \frac{\kappa_1^2}{\mu} + \frac{(\kappa_1+\kappa_2)\gamma^2}{\mu^2}}{(\mathrm{i}a_0)^2 + 2\frac{\gamma}{\mu}\mathrm{i}a_0 + \frac{\kappa_1+\kappa_2}{\mu}} u_0(a_0). \tag{1.37}$$

By equating the coefficients in Equation (1.37) to the terms of the second-order model in Equation (1.27c), the four parameters κ_1, κ_2, γ and μ can be determined. In order to calculate μ, a quadratic equation has to be solved. The quadratic equation for μ is

$$a\mu^2 + b\mu + c = 0 \qquad \text{where} \tag{1.38a}$$

$$a = \alpha_1^4 - 4\alpha_0\alpha_1^2 \tag{1.38b}$$

$$b = -8\alpha_1\beta_1 + 16\beta_0 \tag{1.38c}$$

$$c = 16\frac{\beta_1^2}{\alpha_1^2}. \tag{1.38d}$$

Equation (1.38a) results in two solutions for μ. To ensure real values of μ, $b^2 - 4ac \geq 0$ or $\alpha_0\beta_1^2 - \alpha_1\beta_0\beta_1 + \beta_0^2 \geq 0$. When μ has been determined, the three remaining coefficients can be calculated by

$$\kappa_1 = \frac{\mu\alpha_1^2}{4} - \frac{\beta_1}{\alpha_1} \tag{1.39a}$$

$$\kappa_2 = \mu\alpha_0 - \kappa_1 \tag{1.39b}$$

$$\gamma = \frac{\mu\alpha_1}{2}. \tag{1.39c}$$

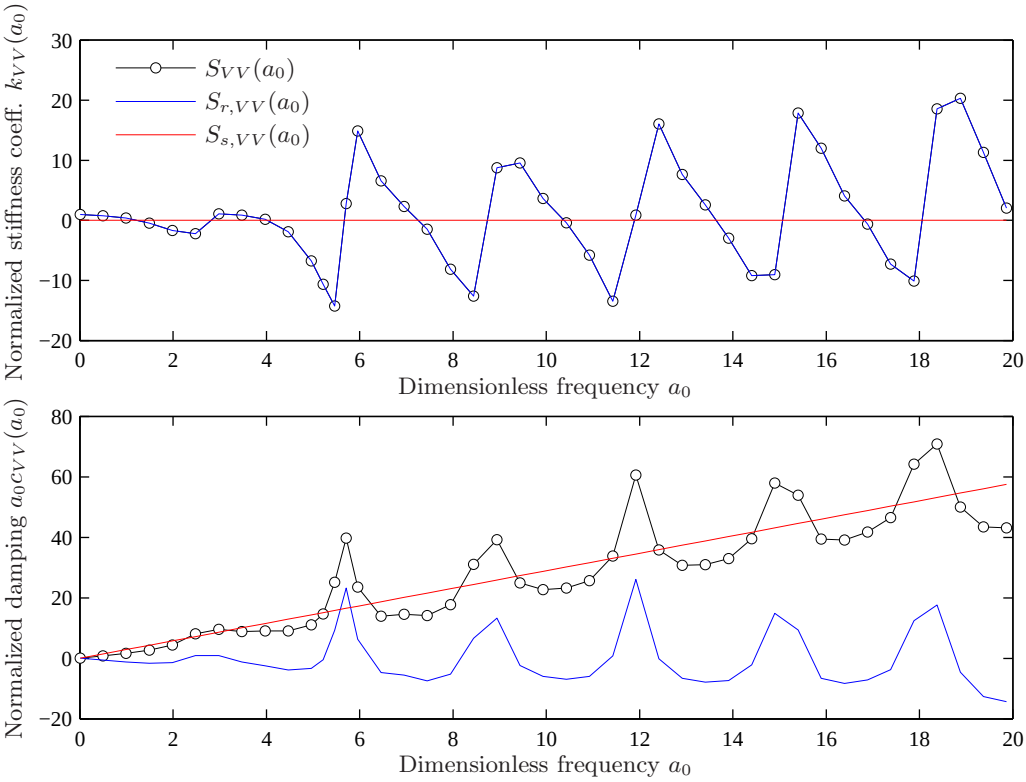

Figure 1.11: Total, regular and singular terms of the vertical dynamic stiffness of a suction caisson. $G_s = 1.0$ MPa, ν_s=1/3.

1.3.5 Example — vertical dynamic stiffness of a suction caisson

Consider a suction caisson with a diameter, $D = 2R$, and the skirt length, H. The vertical dynamic stiffness of the suction caisson has been determined by a three-dimensional coupled boundary element/finite element model, see Section **??** for details. The real and imaginary part of the dynamic stiffness for a suction caisson with $H/D = 1$ is shown in Figure 1.11. The total dynamic stiffness $S_{VV}(a_0)$ is obtained by numerical analysis, and the singular part $S_{s,VV}(a_0)$ is represented by a limiting damping parameter C^{∞}_{VV} that describes the impedance for $a_0 \to \infty$, which in the case of the suction caisson is given by

$$C^{\infty}_{VV} = \rho_s c_P A_{lid} + 2\rho_s c_S A_{skirt}, \tag{1.40}$$

where A_{lid} and A_{skirt} are the vibrating surface areas of the lid and the skirt, respectively. c_P, c_S and ρ_s are the primary (dilatation) wave velocity, shear wave velocity and mass density of the soil, respectively. Finally, the regular part $S_r(a_0)$ is found by subtracting $S_s(a_0)$ from $S(a_0)$, according to Equation (1.17). The real and imaginary part of $S_{VV}(a_0)$, $S_{s,VV}(a_0)$ and $S_r(a_0)$ are illustrated in Figure 1.11

Next, the polynomial-fraction approximation of the regular part $S_r(a_0)$ is applied (Equation 1.22). The polynomial degree of the denominator and the numerator is set to

Table 1.3: Coefficients for the partial-fraction expansion

	Poles s_l	Residues A_l
$l = 1$	$-1.8459 + 6.0094\text{i}$	$-5.6330 - 19.031\text{i}$
$l = 2$	$-1.8459 - 6.0094\text{i}$	$-5.6330 + 19.031\text{i}$
$l = 3$	$-0.2544 + 5.7003\text{i}$	$+0.3581 + 8.1874\text{i}$
$l = 4$	$-0.2544 - 5.7003\text{i}$	$+0.3581 - 8.1874\text{i}$
$l = 5$	$-0.5547 + 2.4330\text{i}$	$-2.1611 + 1.4585\text{i}$
$l = 6$	$-0.5547 - 2.4330\text{i}$	$-2.1611 - 1.4585\text{i}$

6 and 5, respectively. Thus, $2 \times 6 - 1 = 11$ coefficients are to be determined by curve-fitting. The polynomial-fraction approximation is applied for $a_0 \in]0;6]$. The polynomial degree is simply too low to fit the data well for $a_0 \in]0;20]$.

The 11 polynomial coefficients have been determined by curve-fitting (based on least squares method) and converted into a partial-fraction expansion. The results of the curve-fitting are given in table 1.3. It turns out that the partial-fraction expansion of $S_r(\text{i}a_0)$ for this particular foundation is given by three second-order terms, in addition to the singular (const/linear) term. This is due to the fact that the poles and residues of the partial-fraction expansion all are complex. Note that Table 1.3 contains three complex conjugate pairs of poles and residues.

The poles and residues in Table 1.3 are then converted into the appropriate coefficients, according to the expressions in Equation (1.35). The coefficients of the three second-order discrete-elements are shown in Table 1.4.

Table 1.4: Coefficients of the three second-order discrete-elements

	κ_{1l}	γ_{1l}	κ_{2l}	γ_{2l}
$l = 1, 2$	-5.3860	-0.7766	$+3.4420$	$+0.5901$
$l = 3, 4$	$+2.8613$	$+0.0667$	-0.0503	-0.0663
$l = 5, 6$	$+1.5247$	-0.4224	-0.4082	$+0.2366$

The total approximation of the dynamic stiffness can then be formulated by means of Equation (1.26). The coefficients for the three second-order elements are given in Table 1.4, and the last coefficient to be determined is c^∞ of the singular part (if k^∞ vanishes, see Equation (1.19)). c^∞ is found by multiplying Equation (1.40) with $\frac{c_S}{K^0 R}$. In the case c^∞ is equal to 2.8935. All the components have now been determined. The complete lumped-parameter model is shown in Figure 1.12, and the approximation of the total dynamic stiffness $S_{VV}(a_0)$ is shown in Figure 1.13. Note that the approximation fits very well for $a_0 \in]0;6]$, and tends towards the high-frequency limit for $a_0 > 6$. The high-frequency limit corresponds to $S_{s,VV}(a_0)$ in Figure 1.11.

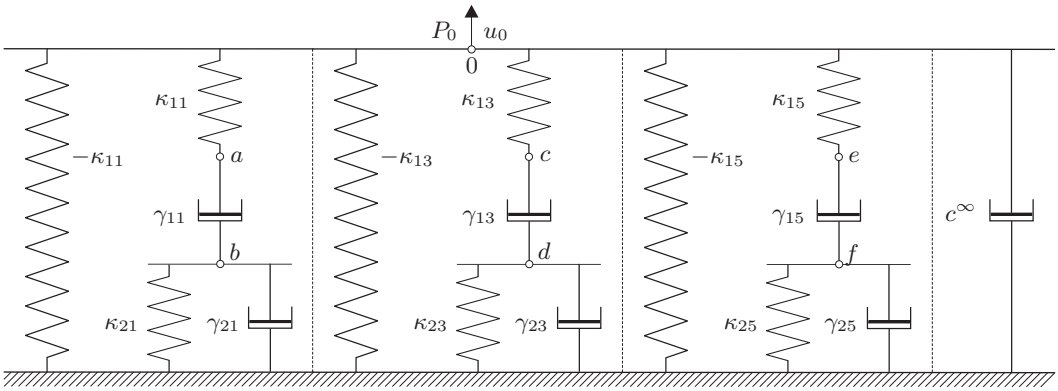

Figure 1.12: Complete lumped-parameter model. The parameters K and $\frac{R}{c_S}K$ are omitted on the κ and γ terms, respectively.

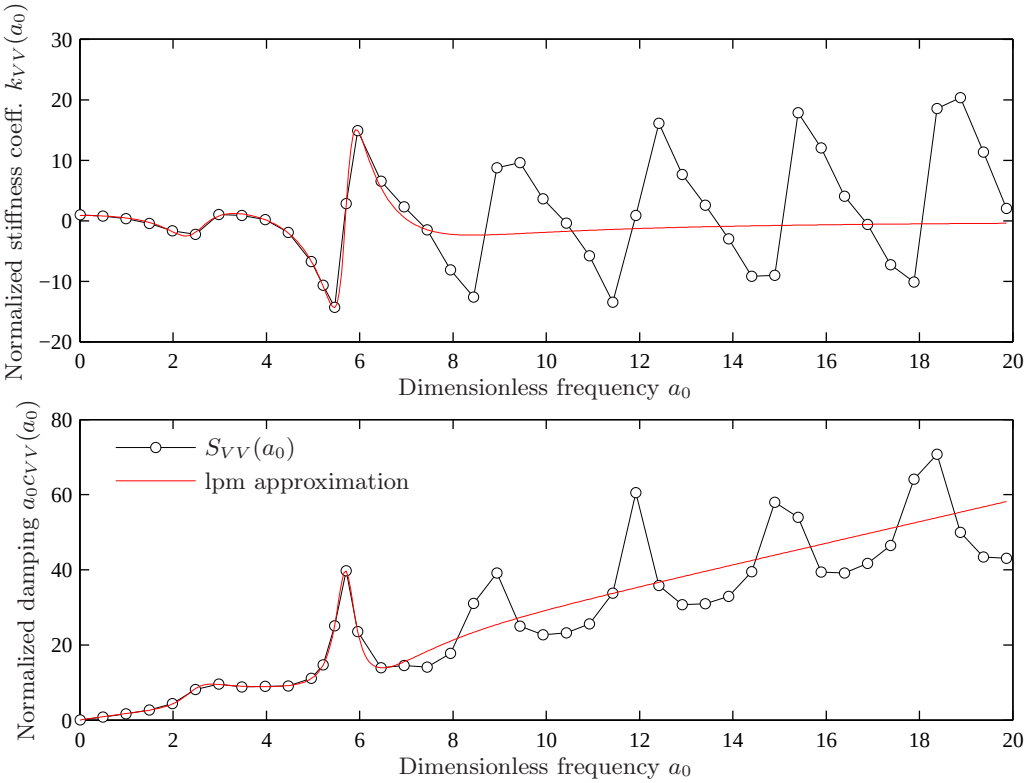

Figure 1.13: Lumped-parameter model approximation of the vertical dynamic stiffness of a suction caisson. The approximation is based on data for $a_0 \in]0;6]$. $G_s = 1.0$ MPa, ν_s=1/3.

Finally, the frequency-independent stiffness and damping matrices of the lumped-parameter model are assembled. There is no mass matrix, since the lumped-parameter model only consists of springs and dampers. The matrices are constructed from the equilibrium equations for each node $(0, a, b, c, d, e, f)$ of the model. The equilibrium formulations (for harmonic loading) are as follows

$$\text{node } 0: \quad [\kappa_{11}K]\left(u_0 - u_a\right) + [-\kappa_{11}K]\,u_0 + [\kappa_{13}K]\left(u_0 - u_c\right) + [-\kappa_{13}K]\,u_0 + [\kappa_{15}K]\left(u_0 - u_e\right) + [-\kappa_{15}K]\,u_0 + \mathrm{i}\omega\left[c^{\infty}\frac{R}{c_S}K\right]u_0 = P_0 \tag{1.41a}$$

$$\text{node } a: \quad [\kappa_{11}K]\left(u_a - u_0\right) + \mathrm{i}\omega\left[\gamma_{11}\frac{R}{c_S}K\right]\left(u_a - u_b\right) = 0 \tag{1.41b}$$

$$\text{node } b: \quad [\kappa_{21}K]\,u_b + \mathrm{i}\omega\left[\gamma_{21}\frac{R}{c_S}K\right]u_b + \mathrm{i}\omega\left[\gamma_{11}\frac{R}{c_S}K\right]\left(u_b - u_a\right) = 0 \tag{1.41c}$$

$$\text{node } c: \quad [\kappa_{13}K]\left(u_c - u_0\right) + \mathrm{i}\omega\left[\gamma_{13}\frac{R}{c_S}K\right]\left(u_c - u_d\right) = 0 \tag{1.41d}$$

$$\text{node } d: \quad [\kappa_{23}K]\,u_d + \mathrm{i}\omega\left[\gamma_{23}\frac{R}{c_S}K\right]u_d + \mathrm{i}\omega\left[\gamma_{13}\frac{R}{c_S}K\right]\left(u_d - u_c\right) = 0 \tag{1.41e}$$

$$\text{node } e: \quad [\kappa_{15}K]\left(u_e - u_0\right) + \mathrm{i}\omega\left[\gamma_{15}\frac{R}{c_S}K\right]\left(u_e - u_f\right) = 0 \tag{1.41f}$$

$$\text{node } f: \quad [\kappa_{25}K]\,u_f + \mathrm{i}\omega\left[\gamma_{25}\frac{R}{c_S}K\right]u_f + \mathrm{i}\omega\left[\gamma_{15}\frac{R}{c_S}K\right]\left(u_f - u_e\right) = 0 \tag{1.41g}$$

By rearranging the the equations with respect to the degrees of freedom, the force-displacement relation for harmonic loading is given by

$$(\mathbf{K} + \mathrm{i}\omega\mathbf{C})\,\mathbf{U} = \mathbf{P}, \tag{1.42}$$

where $\mathbf{K}$, $\mathbf{C}$, $\mathbf{U}$ and $\mathbf{P}$ are given as

$$\mathbf{K} = K \begin{bmatrix} 0 & -\kappa_{11} & 0 & -\kappa_{13} & 0 & -\kappa_{15} & 0 \\ -\kappa_{11} & \kappa_{11} & 0 & 0 & 0 & 0 & 0 \\ 0 & 0 & \kappa_{21} & 0 & 0 & 0 & 0 \\ -\kappa_{13} & 0 & 0 & \kappa_{13} & 0 & 0 & 0 \\ 0 & 0 & 0 & 0 & \kappa_{23} & 0 & 0 \\ -\kappa_{15} & 0 & 0 & 0 & 0 & \kappa_{15} & 0 \\ 0 & 0 & 0 & 0 & 0 & 0 & \kappa_{25} \end{bmatrix} \tag{1.43a}$$

$$\mathbf{C} = \frac{R}{c_S} K \begin{bmatrix} c^{\infty} & 0 & 0 & 0 & 0 & 0 & 0 \\ 0 & \gamma_{11} & -\gamma_{11} & 0 & 0 & 0 & 0 \\ 0 & -\gamma_{11} & \gamma_{11} + \gamma_{21} & 0 & 0 & 0 & 0 \\ 0 & 0 & 0 & \gamma_{13} & -\gamma_{13} & 0 & 0 \\ 0 & 0 & 0 & -\gamma_{13} & \gamma_{13} + \gamma_{23} & 0 & 0 \\ 0 & 0 & 0 & 0 & 0 & \gamma_{15} & -\gamma_{15} \\ 0 & 0 & 0 & 0 & 0 & -\gamma_{15} & \gamma_{15} + \gamma_{25} \end{bmatrix} \tag{1.43b}$$

$$\mathbf{U} = \begin{bmatrix} u_0 \\ u_a \\ u_b \\ u_c \\ u_d \\ u_e \\ u_f \end{bmatrix}, \qquad \mathbf{P} = \begin{bmatrix} P_0 \\ 0 \\ 0 \\ 0 \\ 0 \\ 0 \\ 0 \end{bmatrix} \tag{1.43c}$$

Bibliography

Andersen, L. (2002). *Wave propagation in inifinite structures and media*. PhD thesis, Aalborg University, Denmark.

Beskos, D. E. (1987). Boundary element methods in dynamic analysis. *Appl. Mech. Rev. 40*, 1–23.

Beskos, D. E. (1997). Boundary element methods in dynamic analysis: Part ii (1986-1996). *Appl. Mech. Rev. 50*, 149–197.

Das, B. M. (1993). *Principles of Soil Dynamics*. Pacific Grove, CA, USA: Brooks/Cole.

Domínguez, J. (1993). *Boundary elements in dynamics*. Southampton: Computational Mechanics Publications.

Gazetas, G. and R. Dobry (1984). Simple radiation damping model for piles and footings. *J. Engng. Mech. Div., ASCE 110*(6), 931–956.

Higdon, R. L. (1990). Radiation boundary conditions for elastic wave propagation. *SIAM Journal of Numerical Analysis 27*(4), 831–870.

Higdon, R. L. (1992). Absorbing boundary conditions for acoustic and elastic waves in stratified media. *Journal of Computational Physics 101*, 386–418.

Houlsby, G. and M. Cassidy (2002). A plasticity model for the behaviour of footings on sand under combined loading. *Géotechnique 52*, 117–129.

Krenk, S. (2002). Unified formulation of radiation conditions for the wave equation. *International Journal for Numerical Methods in Engineering 53*(2), 275–295.

Krenk, S. and H. Schmidt (1981). Vibration of an elastic circular plate on an elastic half-space—a direct approach. *Journal of Applied Mechanics 48*, 161–168.

Luco, J. E. and R. A. Westmann (1971). Dynamic response of circular footings. *J. Engng. Mech. Div., ASCE 97*(EM5), 1381–1395.

Martin, C. and G. Houlsby (2001). Combined loading of spudcan foundations on clay: numerical. *Géotechnique 51*, 687–699.

Richart, F. E., J. R. Hall, and R. D. Woods (1970). *Vibration of Soils and Foundations*. Englewood Cliffs, NJ: Prentice-Hall.

Veletsos, A. and Y. Tang (1987). Vertical vibration of ring foundations. *Earthquake Engineering and Structural Dynamics 15*, 1–21.

Veletsos, A. and Y. Wei (1971). Lateral and rocking vibration of footings. *J. Soil Mech. Found. Engrg. Div., ASCE 97*, 1227–1248.

Wolf, J. and A. Paronesso (1991). Errata: Consistent lumped-parameter models for unbounded soil. *Earthquake Engineering and Structural Dynamics 20*, 597–599.

Wolf, J. P. (1991a). Consistent lumped-parameter models for unbounded soil: frequency-independent stiffness, damping and mass matrices. *Earthquake Engineering and Structural Dynamics 20*, 33–41.

Wolf, J. P. (1991b). Consistent lumped-parameter models for unbounded soil: physical representation. *Earthquake Engineering and Structural Dynamics 20*, 11–32.

Wolf, J. P. (1994). *Foundation Vibration Analysis Using Simple Physical Models*. Englewood Cliffs, NJ: Prentice-Hall.

Wolf, J. P. (1997). Spring-dashpot-mass models for foundation vibrations. *Earthquake Engineering and Structural Dynamics 26*(9), 931–949.

Wolf, J. P. and A. Paronesso (1992). Lumped-parameter model for a rigid cylindrical foundation in a soil layer on rigid rock. *Earthquake Engineering and Structural Dynamics 21*, 1021–1038.

Wolf, J. P. and C. Song (1996). *Finite-Element Modeling of Unbounded Media* (1 ed.). Chichester: John Wiley & Sons Ltd.

Wu, W.-H. and W.-H. Lee (2002). Systematic lumped-parameter models for foundations based on polynomial-fraction approximation. *Earthquake Engineering & Structural Dynamics 31*(7), 1383–1412.

Wu, W.-H. and W.-H. Lee (2004). Nested lumped-parameter models for foundation vibrations. *Earthquake Engineering & Structural Dynamics 33*(9), 1051–1058.